Thermodynamic evaluation of the Kalina split-cycle concepts for waste heat recovery applications

Nguyen, Tuong-Van; Knudsen, Thomas; Larsen, Ulrik; Haglind, Fredrik

Published in:
Energy

Link to article, DOI:
10.1016/j.energy.2014.04.060

Publication date:
2014

Thermodynamic evaluation of the Kalina split-cycle concepts for waste heat recovery applications

Tuong-Van Nguyen*, Thomas Knudsen, Ulrik Larsen, Fredrik Haglind

Section of Thermal Energy, Department of Mechanical Engineering, Technical University of Denmark, Building 403, Nils Koppels Allé, 2800 Kongens Lyngby, Denmark

Abstract

The Kalina split-cycle is a thermodynamic process for converting thermal energy into electrical power. It uses an ammonia-water mixture as working fluid (like a conventional Kalina cycle) and has a varying ammonia concentration during the preheating and evaporation steps. This second feature results in an improved match between the heat source and working fluid temperature profiles, decreasing the entropy generation in the heat recovery system. The present work compares the thermodynamic performance of this power cycle with the conventional Kalina process, and investigates the impact of varying boundary conditions by conducting an exergy analysis. The design parameters of each configuration were determined by performing a multi-variable optimisation. The results indicate that the Kalina split-cycle with reheat presents an exergetic efficiency by 2.8 % points higher than a reference Kalina cycle with reheat, and by 4.3 % points without reheat. The cycle efficiency varies by 14 % points for a variation of the exhaust gas temperature of 100 °C, and by 1 % point for a cold water temperature variation of 30 °C. This analysis also pinpoints the large irreversibilities in the low-pressure turbine and condenser, and indicates a reduction of the exergy destruction by about 23 % in the heat recovery system compared to the baseline cycle.

Keywords: Kalina split-cycle, Exergy analysis, Waste Heat Recovery

1. Introduction

The integration of waste heat recovery (WHR) systems in various processes presents thermodynamic and environmental benefits, as it results in a greater power generation for the same fuel input and smaller specific CO_2 emissions. Several power cycles have been suggested in the scientific literature: they differ by the selection of the working fluid, the size of application, the temperature and pressure levels, etc. The most well-known cycles are the steam Rankine cycle, the Organic Rankine cycle (ORC) and the Kalina cycle, in which the working fluid is a mixture of ammonia and water. The two latter cycles are often suggested as alternatives to the steam Rankine cycle for waste heat recovery, as they may display a higher thermodynamic efficiency in low- and medium-temperature applications.

Both power cycles may be viable at the scale of application studied in the present work, i.e. for a net power output of 1-5 MW [1,2]. Victor et al. [3] compared the Kalina cycle and ORC in the temperature range 100-250 °C. It was suggested that, while the two cycles could produce similar power outputs, the ORC was preferable below 200 °C and the Kalina above 200 °C. Wang et al. [4] investigated WHR technologies for use in the cement industry with heat source temperatures of 340 °C. They compared the Kalina cycle and ORC with two steam cycle setups and found that the Kalina cycle had the highest efficiency, followed by the two steam cycles and the ORC. However, Bombarda et al. [5] also compared the Kalina cycle and ORC, for a heat source temperature of 346 °C, and showed that both cycles, when optimised, produced

*Principal corresponding author. Tel.: +45 4525 4129
Email address: tungu@mek.dtu.dk (Tuong-Van Nguyen)

Nomenclature

T	temperature, K	Q	heat
$\bar{e}$	molar exergy, J/mol	W	work
$\dot{E}$	exergy rate, W	ch	chemical
$\dot{Q}$	heat rate, W	ph	physical
$\dot{S}$	entropy rate, W/K	*Subscripts*	
$\dot{W}$	power, W	d	destruction
$\dot{m}$	mass flowrate, kg/s	f	fuel
e	specific exergy, J/kg	j	stream
h	specific total enthalpy, J/kg	k	component
p	pressure, Pa	l	loss
s	specific entropy, J/(kg·K)	p	product
y	component/sub-system exergy ratio	0	dead state
Abbreviations		bub	bubble point
EOS	Equation of State	cv	control volume
ORC	Organic Rankine Cycle	cw	cooling water
WHR	Waste Heat Recovery	dew	dew point
Greek letters		gen	generation
ε	exergy efficiency	in	inlet
Superscripts		out	outlet
*	relative	r	rich ammonia concentration

almost equal net power outputs. The present study does not directly compare the ORC with the Kalina cycle but is based on the boundary conditions used in the work of Bombarda et al. [5], to allow further evaluations of the power cycle performance.

Energy can neither be created nor destroyed, and an energy analysis illustrates the energy transformations and flows throughout the system under study. On the opposite, exergy is not conserved in any real process, illustrating therefore the locations, causes and magnitudes of the thermodynamic irreversibilities taking place. Exergy destruction also accounts for the additional exergetic fuel required because of the system imperfections. Several studies on the thermodynamic performance of the Kalina cycle exist. Marston [6] carried out a parametric study of the Kalina cycle. The turbine inlet composition and separator temperature were identified as the key parameters to optimise. These findings were supported by Nag and Gupta [7], who performed an exergetic analysis of the Kalina cycle, and identified the turbine inlet temperature and composition, as well as the separator temperature, as having the largest influence on the thermodynamic performance of this cycle. Dejfors and Svedberg [8] conducted an exergy analysis to compare the Kalina cycle with a steam Rankine cycle for a direct fired biomass-fueled cogeneration plant. They noted that the aspect of being direct fired lead to significantly higher exergy losses in the boiler for the Kalina cycle compared to the Rankine cycle. Jonsson [9] investigated the Kalina cycle as WHR system for gas engines and gas diesel engines. It was argued that the Kalina cycle presents the potential to generate more power than the steam Rankine cycle, and that the additional costs could be justified by the gains in efficiency. Singh and Kaushik [10] investigated a Kalina cycle coupled to a coal fired steam power plant. They identified the primary source of exergy destruction, and therefore the greatest potential for optimisation, as the boiler.

The present paper presents and evaluates a unique power generation cycle, called the Kalina split-cycle. This process is also based on the ammonia-water mixture as working fluid, like the conventional Kalina cycle, but is characterised by a varying ammonia concentration in the heat recovery system. This can result in a smaller entropy generation in the heat transfer process, and potentially in a higher exergetic efficiency of the complete power cycle. This concept was briefly mentioned in the work of Kalina [11].

In the system analysis presented in Larsen et al. [12], it was suggested that the components that affect the process efficiency and optimisation the most are the separator, the recuperators, the boiler and the turbine. Moreover, it was indicated that the most important variables that impact the thermal efficiency are the ammonia concentration and the cooling water temperature. A simplified cost analysis of the Kalina split-cycle was also conducted, and the payback time of this particular process layout is sensibly similar to the payback time of a conventional Kalina cycle. The major costs were related to the boiler and turbines. The boiler costs are estimated to be about 40 % higher if the Kalina split-cycle with reheat is compared to the conventional Kalina cycle, and about 45 % if compared to the Kalina cycle with reheat. The turbine costs are estimated to be about 30 % higher if the Kalina split-cycle with reheat is compared to the conventional Kalina cycle, and about 6 % if compared to the Kalina cycle with reheat.

The literature appears to contain little on the thermodynamic performance of such cycles, and this study aims at closing this gap, following these three objectives:

- estimation of the cycle potential, in terms of exergy efficiencies, economic costs and environmental impacts, compared to a conventional Kalina cycle, with and without reheat;
- analysis of the plant inefficiencies and of the exergy destruction trends;
- evaluation of the effect of the boundary conditions (heat source and cold reservoir temperatures) on the system performance.

Section 2 presents the design of the Kalina split-cycle system and the methods used in this work are reported in Section 3. The results are presented in Section 4 and concluding remarks are outlined in Section 5.

2. System description

2.1. Reference Kalina cycle

The Kalina cycle is similar in principle to the Rankine cycle, in which heat is supplied to a closed process loop, and where thermal energy is converted into mechanical work. The main difference lies in the properties of the working fluid, which is an ammonia-water mixture in the Kalina cycle. This two-component mixture is zeotropic, which means that the vapour and liquid phases do not have the same composition when condensation and evaporation take place. At constant pressure, the evaporation temperature changes during the heat transfer process, unlike pure substances, which have a constant evaporation temperature. The temperature glide results in a better match between the temperature profiles of the heat source and receiver. The exergy destruction caused by the heat transfer process is therefore smaller, but the area requirements of the heat exchangers increase. The range of the temperature glide can be adjusted by modifying the ammonia and water fractions of the working solution, as well as the operating pressure. The Kalina cycle may therefore be suitable for both low- and medium-temperature heat recovery applications. Several configurations of this thermodynamic cycle exist. The layout considered in this work is inspired by the one presented in the study of Bombarda et al. [5] and was studied by Marston [6,13] and El-Sayed [14]. The terms 'rich' and 'lean' imply ammonia-rich and ammonia-lean in the rest of this work. Four different ammonia concentrations can be found in the conventional Kalina cycle.

2.2. Kalina split-cycle

The Kalina split-cycle (Figure 1) is fundamentally similar to the Kalina cycle, both using the ammonia-water mixture. The main difference lies in the change of ammonia concentration in the evaporation process, which involves a more complex splitting and mixing arrangement to achieve the desired ammonia concentrations. Five different concentrations can be found in the Kalina split-cycle and are denoted 'very rich' (points 18, 19 and 26), 'rich' (points 20 to 25, and 33) , 'basic' (points 1 to 5), 'lean' (points 27 to 32), and 'very lean' (points 11 to 16), in reference to their ammonia content.

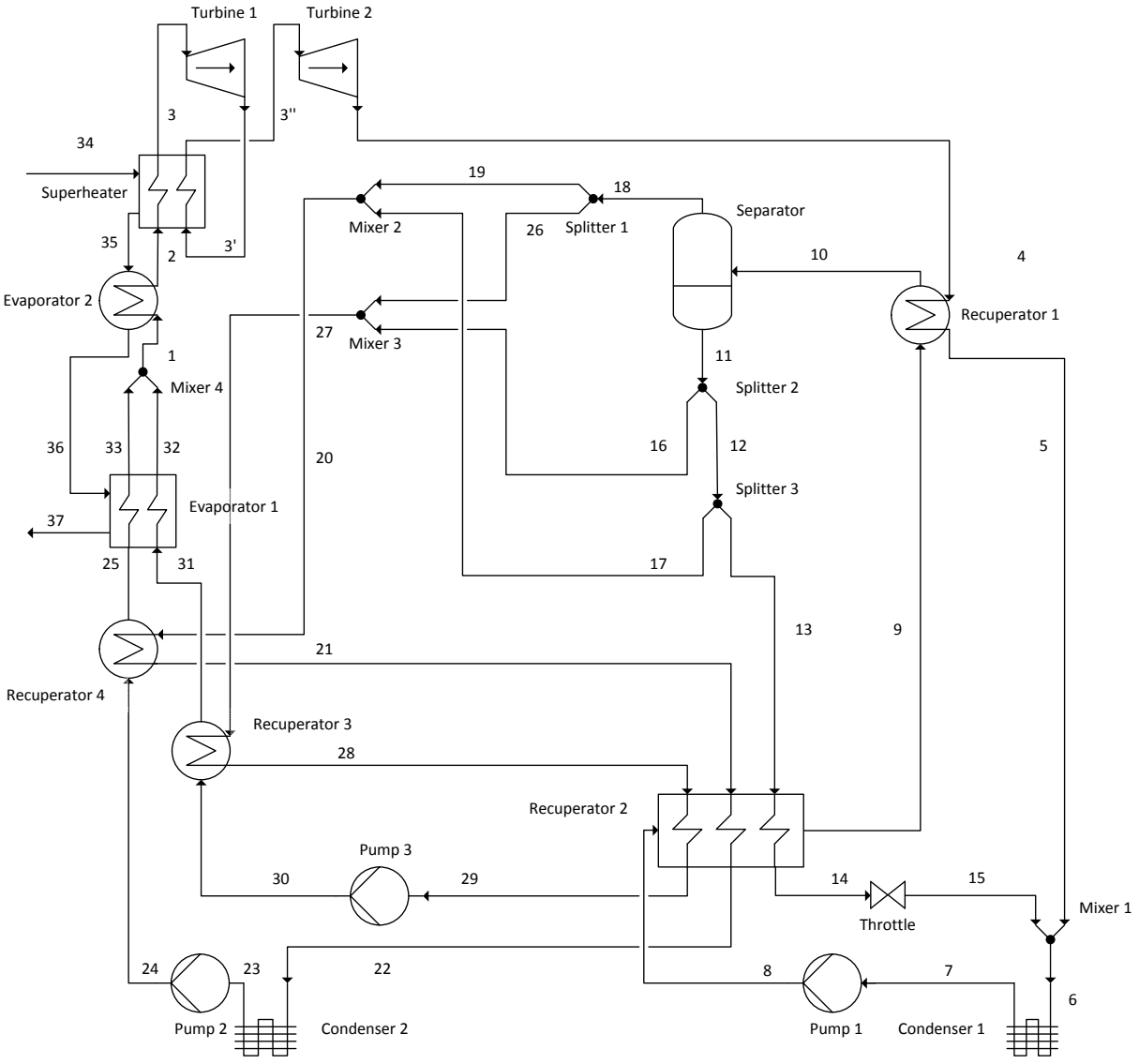

Figure 1: Flowchart of the Kalina split-cycle process

At the difference of the Kalina cycle where there is only one single stream, two streams with different ammonia concentration enter the boiler, an ammonia-rich (25) and an ammonia-lean (31). In the boiler, the former is fully evaporated (33) while the latter stays in liquid form, but is heated to its bubble point temperature (32). They are then mixed into (1): the resulting solution is an ammonia-water solution in vapour-liquid equilibrium, which is evaporated (2) and superheated (3). The benefits of splitting the streams can be visualised in temperature-enthalpy diagrams shown in Larsen et al. [12].

In all cases, the minimum temperature difference, i.e. the pinch point location, is found in the evaporation process, i.e after the preheating and before the mixing of the rich and lean streams. This work assumes that the rich and lean streams are mixed at the same temperature and pressure to reduce the entropy generation due to mixing effects. In addition, Kalina [11] suggested that the rich stream should be at its dew point, while the lean stream should be at its bubble point. The vapour and liquid phases of each stream are therefore at their equilibrium concentrations, which minimises the entropy generation in the mixing process. However, such constraint fixes the mixing temperature, as the ammonia concentration of the lean and rich streams are interdependent. The actual mixing point has little influence on the overall performance of the system, since the pinch point is indeed located either at the bubble temperature of the ammonia-rich stream or at the outlet of the superheater T_3.

3. Methods

3.1. Modelling and simulation

This study was built on a baseline case adapted from the work of Bombarda et al. [5], where the integration of a bottoming Kalina cycle was studied, using exhaust gases from diesel engines as heat source. The Kalina cycle was compared to the Kalina split-cycle, considering one reheat stage as a possible option, and the models were validated in [12]. The full power cycle was simulated using both Matlab [15] and Aspen Plus® [16], based on the equations of state derived from Tillner-Roth and Friend (REFPROP) [17] to estimate the physical and thermodynamic properties.

The modelling of the Kalina split-cycle considered the same assumptions as presented in Bombarda et al. [5], at first for comparing the performance of this alternative configuration to the more conventional one (Table 1). The waste heat source was exhaust gases from marine diesel engines with a total flowrate of 35 kg/s, inlet and outlet temperatures of the waste heat recovery boiler of 346 °C and 127.7 °C, and a composition of 74.6 % N_2, 11.7 % O_2, 6.7 % H_2O, 5.9 % CO_2 and 1.1 % Ar on a molar basis.

Table 1: System parameters (baseline case)

Parameter	Description	Value
T_{34}	Heat source inlet temperature	346 °C
T_{37}	Heat source outlet temperature	127.7 °C
T_{cw}	Cooling water inlet temperature	25 °C
$T_{34} - T_3$	Superheater approach	16 °C
ΔT_{evap}	Minimum temperature difference (boiler)	21.9 °C
ΔT_{rec}	Minimum temperature difference (recuperators)	5 °C
ΔT_{cond}	Minimum temperature difference (condenser)	4.5 °C
$\eta_{t,\mathrm{pol}}$	Turbine polytropic efficiency	70.5 %
$\eta_{t,\mathrm{mec}}$	Turbine mechanical efficiency	96 %
η_{pp}	Pump efficiency	70 %
η_{dr}	Driver efficiency	95 %

A multi-level approach was applied to model and optimise the two main sub-systems of the power cycle, which were namely (i) the split-cycle boiler and turbine sub-system, where the optimal boiler *pressure* and *inlet temperature* on the working fluid side were determined, and (ii) the mixing and splitting arrangement, where the *split fractions* and corresponding *flow rates* were calculated to reach the desired ammonia concentrations of the working mixtures.

3.1.1. Thermodynamic level - sub-modelling

The prediction of the thermophysical properties of the ammonia-water mixture builds on the model developed by Tillner-Roth and Friend. This equation of state is applicable in the liquid and vapour phase regions and is suitable for predicting the vapour-liquid equilibrium [17]. The main difference with the other equations of state used for ammonia-water mixtures (Stecco-Desideri and Ibrahim and Klein) lies in the addition of a correction term to the ideal mixture behaviour in the EOS, making this EOS suitable for pressures up to 40 MPa. This EOS was compared to the two others in a work of Thorin [18] and is more accurate, which is of particular importance as the value of the thermal efficiency can vary up to 1.5 %

points when using different EOS. However, this EOS is characterised by a significantly higher computational time than conventional cubic EOS such as Peng-Robinson or Redlich-Kwong with Soave modifications, but presents a better accuracy.

3.1.2. Subsystem level - sub-modelling

The division of a system into its sub-systems eased the initialisation of the state and operating parameters for performing the optimisation procedure, and the two sub-models were validated by using equivalent models in Aspen PLUS [19].

Heat exchanger sub-system. A model of the boiler was developed, based on the initial waste heat source conditions given in Bombarda et al. [5], in order to analyse the entropy generation trends. As the power output is proportional to the flow rate of the working fluid flowing through the boiler, the aim is to determine correlations between the maximum possible flow rate and the compositions of the lean and rich streams. The composition of the lean stream is linked to the composition of the rich one, since (i) the temperatures and pressures of these streams are equal at the outlet of the first evaporator, and (ii) the rich stream is in saturated vapour state and the lean stream is in saturated liquid state. The optimisation bases therefore on a computation of the rich stream composition against the mass flow rate of the working fluid, under these three constraints suggested by Kalina [11]:

$$T_{\text{dew,rich}} = T(p = p_{\text{wf}}, Q = 1, x = x_{\text{rich}}) \tag{1}$$

$$T_{\text{bub,lean}} = T(p = p_{\text{wf}}, Q = 0, x = x_{\text{lean}}) \tag{2}$$

$$T_{\text{dew,rich}} - T_{\text{bub,lean}} = 0 \tag{3}$$

Mixing and splitting sub-system. The aim of this model is to calculate the necessary splitting fractions to achieve the desired flows and concentrations of the lean and rich streams entering the boiler, based on the temperature and pressure conditions at the flash separator inlet. This separation is assumed adiabatic. The coupling of these two models allows for a sound and computationally more-efficient optimisation of the Kalina Split Cycle, under fixed boundary conditions.

3.1.3. Optimisation

These models were further integrated into a model of the complete system to investigate its feasibility. The optimisation was carried out using a genetic algorithm [12]: the optimisation parameters (process variables) are emulated, as if they were genes of an individual, and the performance of each individual is evaluated. The objective of the optimisation routine is to maximise the net power production, considering nine process parameters as decision variables:

- temperature T_{10}, pressure p_{10} and concentration x_{10} of the working mixture at the inlet of the separation sub-system;
- working solution concentration x_3;
- turbine inlet p_3, reheat $p_{3'}$ and outlet p_4 pressures;
- boiler temperature approach;
- rich stream concentration x_{20}.

The discharge temperature and mass flow rate of the heat source are kept constant, implying that maximising the net power output is equivalent to maximising the thermal efficiency of the Kalina split-cycle. The first generation of individuals is randomly generated, while the next ones are stochastically selected based on the values of the optimisation function. The following generations are used in the next iteration of the genetic algorithm, resulting in sets of best possible combinations of process parameters. The initial population size is set to 400-800, the number of generations is 30 and the number of evaluations

between 12,000 and 24,000, to ensure that the global optimum is found in a search space where several local optima are present. The number of sub- populations, the cross-over rate and the generation gap are set to 4, 1 and 0.8, while the mutation, insertion and migration rates are set to 0.5, 0.9 and 0.2. The MATLAB GA-toolbox was used to perform the optimisations.

3.2. System analysis

3.2.1. Strategy

The study performed in this work can be divided into five consecutive steps:

1. the Kalina split-cycle is compared to the conventional Kalina and organic Rankine cycles, with the working fluid and boundary conditions proposed in Bombarda et al. [5], in order to have a comprehensive overview of the differences between the various waste heat recovery cycles;

2. four configurations of the Kalina cycle and split-cycle were studied (denoted *Case A* for the Kalina cycle without reheat, *Case B* for the Kalina cycle with reheat, *Case C* for the Kalina split-cycle without reheat, and *Case D* for the Kalina split-cycle with reheat) to deduce further optimisation possibilities;

3. a sensitivity analysis on the performance of the Kalina split-cycle for nine boundary conditions was conducted (Table 2). The efficiency of this power cycle in other ambient conditions was investigated by varying the cooling water temperature, and the suitability to low- and medium-temperature applications was studied by changing the hot source inlet temperature. The effect of lower exhaust temperatures was considered, starting from a temperature of 160 °C to 100 °C, with a step of 15 °C. Exhaust temperatures of 100 °C are currently not achievable because of practical issues with possible sulphur condensation in the fumes, resulting in material corrosion in the chimneys. They may be adequate in the future for fuels with a low sulphur content, natural gas, or with the development of new technologies;

4. the relationship between the ammonia mass fraction and the exergy flows, as well as with the distribution of the exergy destruction, is investigated. The ammonia mass fraction is varied between 0.7 and 0.8 with a step of 0.05. The high pressure is kept constant, meaning that the process parameters that vary are the mass flow rate, the intermediate and low pressure levels, and the split fractions in the mixing/separation system;

5. the entropy generation phenomenon inside the boiler is analysed by discretization of the heat exchangers of the Kalina split-cycle in finite control volumes.

Table 2: Sensitivity boundary conditions

#	T_{34} [°C]	T_{37} [°C]	T_{cw} [°C]
1	350	160	40
2	350	160	25
3	350	160	10
4	300	160	25
5	250	160	25
6	350	100	25
7	350	115	25
8	350	130	25
9	350	145	25

3.2.2. Thermodynamic analysis

Exergy may be defined as the *maximum theoretical useful work as the system is brought into complete thermodynamic equilibrium with the thermodynamic environment while the system interacts with this environment only* [20]. Exergy is not conserved in real processes as it is destroyed because of internal irreversibilities.

Neglecting the potential and kinetic effects, the exergy associated with a stream of matter is a function of its physical e^{ph} and chemical e^{ch} components [20]. It is expressed, on a specific mass basis, as follows:

$$e = e^{\mathrm{ph}} + e^{\mathrm{ch}} \tag{4}$$

Physical exergy accounts for temperature and pressure differences from the environmental conditions and is defined as:

$$e^{\mathrm{ph}} = (h - h_0) - T_0(s - s_0) \tag{5}$$

where s is the specific entropy of a stream of matter per unit-of-mass, respectively.

Chemical exergy accounts for deviations in chemical composition from reference substances present in the environment. In this work, chemical exergy is calculated based on the concept of *standard chemical exergy* discussed by Moran and Shapiro [21]. The specific chemical exergy of real chemical compounds is determined using the reference environment defined by Szargut [22–24].

The tracing of the energy and exergy flows provides information on the system transformations and inefficiencies. Several performance parameters were developed to illustrate the possibilities for improvements and illustrate the components on which improvement efforts should focus [20,25–27]:

- The exergy destruction ratio y_d^* is defined as the ratio of the exergy destruction rate $\dot{E}_{d,k}$ within a specific component k to the total exergy destruction rate in the overall system $\dot{E}_d$:

$$y_d^* = \frac{\dot{E}_{d,k}}{\dot{E}_d} \tag{6}$$

- The exergetic efficiency ε of a given component or sub-system k, which reflects its thermodynamic performance. It is defined as the ratio of the product exergy to the fuel exergy.

$$\varepsilon_k = \frac{\dot{E}_{p,k}}{\dot{E}_{f,k}} = 1 - \frac{\dot{E}_{d,k}}{\dot{E}_{f,k}} \tag{7}$$

  The product exergy $\dot{E}_{p,k}$ represents the desired effect of a given thermodynamic transformation or process, while the fuel exergy $\dot{E}_{f,k}$ represents the resources expended in this component/sub-system to generate the desired result. The definitions of exergetic fuels and products for the components existing in power cycle processes are introduced and discussed in Kotas [25–27] and in Bejan et al. [20]. The exergy losses with cooling water and exhaust gases cannot be allocated to a single component, but rather to the complete system, and are therefore not accounted for in the definition of the exergy efficiency of a component.

The exergy accounting for the Kalina split-cycle can therefore be expressed as follows:

$$\dot{E}^Q_{\mathrm{heat}} = \dot{E}^W + \dot{E}^Q_{\mathrm{cw}} + \dot{E}^Q_{\mathrm{exh}} + \dot{E}_d \tag{8}$$

where $\dot{E}^Q_{\mathrm{heat}}$ represents the exergy input to the power cycle with the heat source, $\dot{E}^W$ denotes the exergy associated with the net power produced, $\dot{E}^Q_{\mathrm{cw}}$ and $\dot{E}^Q_{\mathrm{exh}}$ the exergy lost to the environment with the cooling water and exhaust gases, and $\dot{E}_d$ the exergy destroyed in the plant. The dead state was taken to the environmental conditions, i.e. 5 °C and 1.013 bar, and the reference environment of Szargut [28] is considered for the chemical exergy calculations.

3.2.3. Economic analysis

An economic and a life cycle assessment are performed to further compare the three cycles, i.e. the organic Rankine cycle, Kalina cycle and Kalina split-cycle. The grassroot costs are estimated from the capacity-based correlations, based on design and operating parameters such as the heat transfer area, the thermal and power loads, and they are characterised by an uncertainty of ± 30 %. The estimates of the heat transfer areas were taken from Larsen et al. [12]. For more details on the used correlations, the reader is referred to Turton et al. [29]. The interest rate is set to 6 % and the lifetime of the equipment to 15 years.

3.2.4. Life cycle analysis

The environmental impacts of integrating waste heat recovery cycles are estimated by taking into consideration the environmental burdens during the whole life cycle, including the manufacturing, operating and decommissioning steps, and by applying the approach of Gerber et al. [30]. The impacts are normalised with respect to the functional unit of the power cycle, which is, in this work, taken to be 1 GJ of electricity, and they are adjusted for an operating availability of 95 %. The environmental effects that are investigated are, namely, the global warming potential, over a horizon of 100 years, the ozone depletion potential, the acidification and eutrophication effects, the human toxicity and the marine ecotoxicity. The pollutant emissions are indexed on the CO_2, CFC-11, SO_2, PO_4^- and 1,4-DCEB compounds.

4. Results and discussion

4.1. Comparison of the Organic Rankine Cycle, Kalina Cycle and Kalina Split Cycle

The Organic Rankine cycle, with the boundary conditions, the process parameters and the working fluid suggested in Bombarda et al. [5], is compared to the Kalina cycle and the Kalina split-cycle. It should be mentioned that the Organic Rankine cycle proposed in their work considers an organic fluid operated in subcritical conditions, and that there could be more efficient and optimised cycles with fluids operating in supercritical ones. However, such an investigation is out of scope of this study, and this comparison aims at illustrating the most important differences between the three cycles.

Table 3: Comparison of the Organic Rankine cycle, Kalina cycle and Kalina split-cycle, based on thermodynamic, economic and environmental performance indicators.

	Organic Rankine cycle (hexamethyldisiloxane)	Kalina cycle without reheat	Kalina split-cycle with reheat
Thermodynamic evaluation			
Net power generation, kW	1603	1753	1910
Thermal efficiency, %	21.5	23.6	25.7
Low pressure, bar	0.12	6.5	4.9
High pressure, bar	9.74	150	125.1
Economic assessment			
Total grassroot costs, M$	8.14	9.99	11.31
Recuperators, %	2.84	4.43	5.18
Condensers, %	1.99	3.32	3.01
Boiler, %	13.81	21.02	27.04
Separator, %	-	0.66	0.40
Pumps, %	1.96	4.20	6.01
Turbine, %	79.41	66.36	58.36
Production cost, $/MWh	61.6	71.1	80.9
Environmental impacts			
Acidification, kg SO_2-eq	-0.07	-0.069	-0.068
Eutrophication, 10^{-3} kg PO_4-eq	-6.50	-6.40	-6.25
Global warming potential, kg CO_2-eq	-58	-58	-59
Ozone depletion, 10^{-6} kg CFC11-eq	-2.20	-2.10	-2.15

The Kalina split-cycle is characterised by greater grassroot costs, as the number of components in this configuration is much higher than for a conventional Kalina cycle, and thus even higher than for an Organic Rankine cycle. This main increase of costs can be imputed to the greater complexity of the boiler, as streams of different concentrations should be handled separately. Despite the higher thermal efficiency of this power cycle, the total and production costs are 30-40 % higher compared to an Organic Rankinecycle, and the

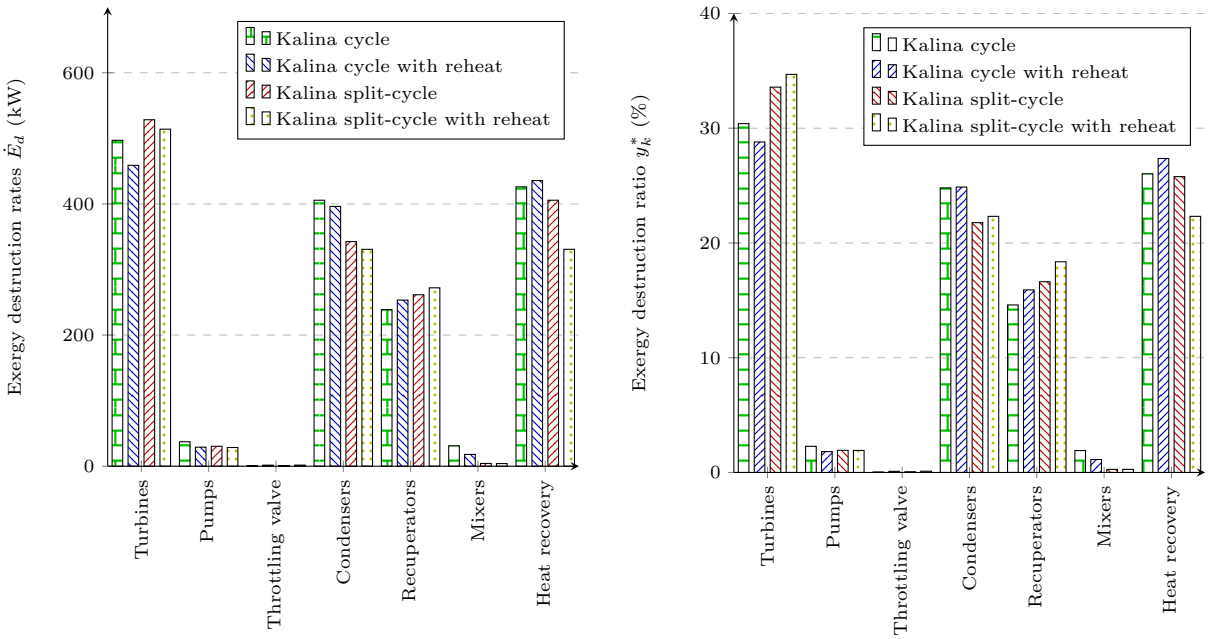

Figure 2: Comparison of the exergy destruction rates and exergy destruction ratios in the four Kalina cycle configurations (Kalina cycle (Case A), Kalina cycle with reheat (Case B), Kalina split-cycle (Case C), Kalina split-cycle with reheat (Case D)). The exergy losses associated with the rejection of the exhaust gases are not shown, since they are equal in the four cases.

pumps and turbines operate over larger pressure ratios (Table 3). Integrating a waste heat recovery cycle has overall positive environmental effects, as electricity from the grid is substituted. The emissions caused by the component construction, maintenance and operation are compensated by the reduction in most pollutants emissions, with the exception of the ones contributing to human toxicity and marine ecotoxicity.

4.2. Comparison of the 4 configurations

The exergy destruction in the Kalina cycle amount to 1726 kW (*Case A*), 1681 kW (*Case B*), 1662 kW (*Case C*) and 1575 kW (*Case D*). The exergy efficiencies are 26.5 %, 27.5 %, 27.0 % and 28.9 %, respectively. The exergy analysis indicates that the implementation of the reheat and split-cycle configurations result in reduced exergy destruction and losses by 2.5–4.9 % and 2.7–5.1 % (Figure 2). In all cases, the greatest irreversibilities take place (1) in the turbine(s), (2) in the heat recovery system, and (3) in the condensers and recuperators.

The Kalina split-cycle is characterised by a significant reduction of the exergy destruction in heat transfer processes, mainly because most desuperheating of the rich stream takes place in the recuperators, rather than in the intermediate pressure condenser (36–38 % in relation to the baseline case) and heat recovery system (4.8–24 %). In contrast, the exergy destruction in the recuperators is higher, because more heat is transferred in these heat exchangers. The exergy losses associated with the rejection of the exhaust gases to the environment are constant and equal to 5640 kW, since the comparison of the four Kalina cycle configurations is based on fixed temperature and pressure of the exhaust gases at the outlet of the heat recovery system. On the contrary, the exergy losses with the cooling water are slightly higher in the Kalina split-cycle cases.

The Sankey diagram of the Kalina split-cycle with reheat (Figure 3) illustrates graphically the exergy flows within the plant, as well as the main sources of inefficiencies and losses. The greatest exergy destruction take place in (i) the low-pressure turbine, (ii) the boiler, (iii) the condenser of the lean mixture, and (iv) the recuperator placed at the outlet of the turbines. The other contributions are moderate in comparison, accounting for less than 100 kW each. The irreversibilities corresponding to the point (i) are related to the inefficiencies of the low-pressure turbine, which is characterised by a significant pressure ratio. The ones

corresponding to the points (ii), (iii) and (iv) are caused by the heat transfer from the exhaust gases to the working mixture, and from the working mixture to the cooling water.

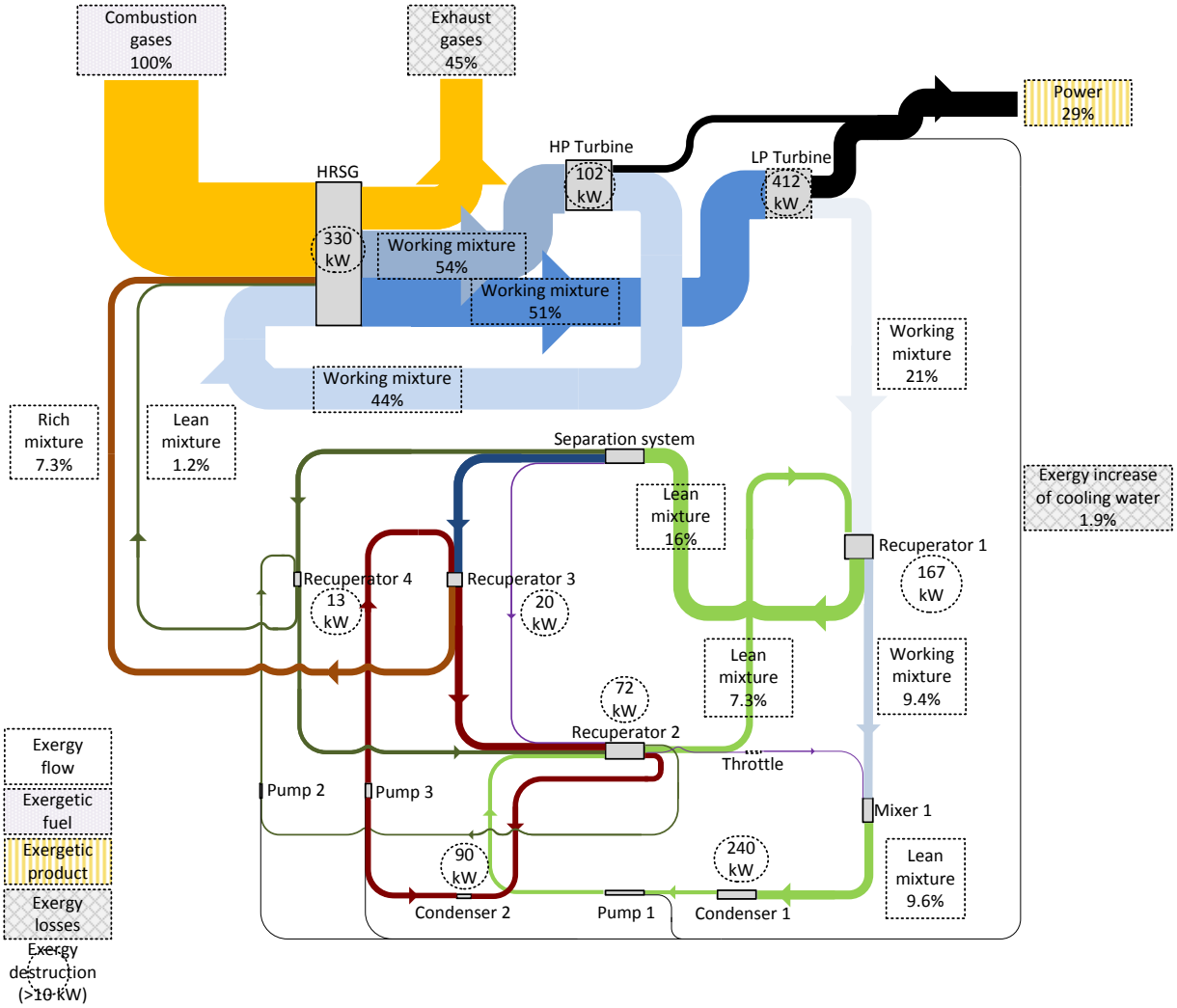

Figure 3: Sankey diagram of the Kalina split-cycle process with reheat. The arrangement of mixers and splitters to reach the desired ammonia and water concentrations in the rich and lean fluids is represented graphically as the separation system. Only the irreversibilities greater than 10 kW are shown, and the exergy accounting on the diagram considers that the exergy destruction caused by chemical mixing is negligible towards the other contributions and the physical exergy of each material stream.

4.3. Effect of the boundary conditions

The optimisation results for the sensitivity analysis presented in Table 2 are shown in Table 4. It suggests that there is no direct correlation between the optimum mass flow rate and the temperature of the environment. Lower cooling water temperatures result in higher optimal high pressure levels, as well as lower condensation temperatures of the working mixture. The ammonia fraction can therefore be increased, which results in a greater power output. Higher exhaust temperatures result in smaller working mixture flow rates, as well as higher high pressure levels, since a smaller amount of heat can be recovered in the waste heat recovery system.

Table 4: Optimum design parameters, net power generation and exergetic efficiency of the Kalina split-cycle at different boundary conditions.

#	$\dot{m}$	p_3	p_{10}	p_4	x_a	$\dot{W}$	ε
1	3.31	127	13.9	4.3	0.634	1694	28.5
2	3.14	126.8	11.2	3.2	0.671	1813	28.2
3	3.45	129.5	9.9	3.5	0.754	1939	27.6
4	2.85	128.7	12.1	6.2	0.766	1211	21.9
5	1.90	65.4	11.4	4	0.657	668.5	14.5
6	3.96	62.7	10.8	2.9	0.685	2055	31.8
7	3.78	70.9	10.2	2.8	0.663	2027	31.2
8	3.78	101	10.4	3.6	0.692	2006	30.8
9	3.36	125.4	9.5	3	0.691	1974	30.4

The net power generation of the Kalina split-cycle is mostly sensitive (i) to the cooling water temperature, increasing by about 7 % for a decrement of 15 °C, and (ii) to the inlet temperature of the waste heat source, decreasing by about 40 % for a reduction of 50 °C. Similarly, the exergy efficiency of this power cycle is very sensitive to the waste heat temperatures, while it is moderately changing with the cooling water and exhaust gas temperatures (Table 4).

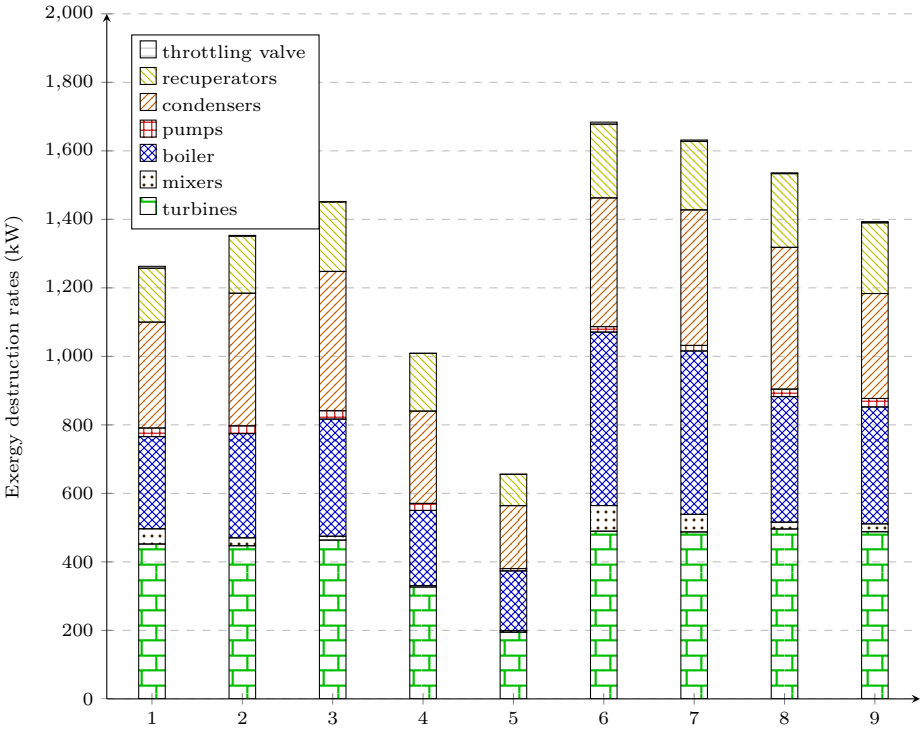

Figure 4: Exergy destruction sorted by processes, under different boundary conditions (temperatures of the heat source, heat rejection and cooling water).

The greatest exergy destruction can be found in the turbines, boiler and condenser, while the irreversibilities taking place in the mixers, pumps and throttling valves are negligible (Figure 4). The turbines are the most exergy-destroying system for all cases investigated in this work, with the exception of Case 6 where the boiler ranks first. This can be explained by the larger temperature difference between the inlet and outlet temperatures on the gas side, implying that the exergy destruction caused by heat transfer is higher.

When investigating each individual component, it can be seen that the boiler and the high- and low-pressure turbines are generally the most exergy-destroying components (Figure 5), although they also display the highest exergy efficiency, of 87–91 %, 80–84 % and 78–81 %, respectively. This high value is related

to the improved match between the temperature profiles of the heat source and receiver. However, the boiler is also responsible for large exergy destruction, as the total flow rate of the working solution flows through this component, and heat transfer takes place over a large range of temperatures. The low-pressure condenser and high-pressure turbine rank third or fourth most exergy-destroying component in all cases, as large amounts of exergy are transferred at low temperatures and the high-pressure turbine operates over a large pressure ratio.

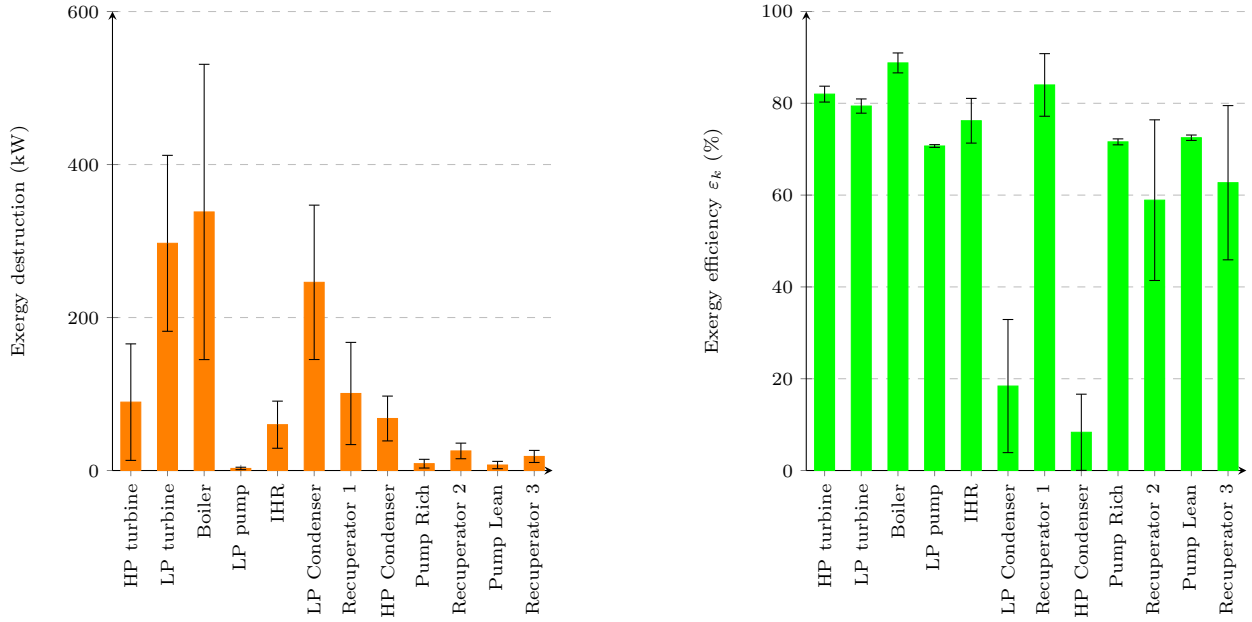

Figure 5: Exergy destruction sorted per component (left), under different boundary conditions (temperatures of the heat source, heat rejection and cooling water). Exergy efficiency per component ε_k (right), under different boundary conditions (temperatures of the heat source, heat rejection and cooling water). The range indication represents the minimum and maximum values for the specific component across the examined cases.

The pumps destroy little exergy and present an efficiency of about 70 %. The first and second recuperators, where heat is recovered from the turbine effluent, are more efficient by 10–15 % points than the third and fourth recuperators, where the rich and lean working fluids are preheated before entering the boiler.

The exergy losses with cooling water are negligible in comparison to the ones associated with exhaust gases. The latter decrease with the limit set on the exhaust temperature, from about 3500 to 2050 kW when it decreases from 160 °C to 100 °C.

The exergy destruction taking place in the turbines vary significantly with the boundary conditions, while their exergetic efficiencies change marginally. This suggests that the variations of the exergy destruction in these components are mostly correlated to (i) the variations of the pressure ratios of the high- and low-pressure turbines, and to (ii) the variations of the working mixture flow rates. On the opposite, the exergy efficiency of the condensers is directly impacted by changes in the cooling water temperature, as exergy is dumped into the environment at low temperatures. Similarly, the exergy efficiency of the recuperators is affected by the exhaust temperature, as this results in different operating conditions of the recuperators, and therefore in different temperature gaps between the hot and cold streams.

4.4. Effect of the ammonia mass fraction

The relation between the ammonia mass fraction and the exergy flows entering the several components, as well as their exergy destruction and efficiency, are investigated. The ammonia mass fraction is fixed to 0.7, 0.75 and 0.8, while the high pressure is kept constant and the other process parameters (e.g. mass flow rate) are taken as decision variables in the optimisation routine. For the same boundary conditions, the

total exergy destruction in the Kalina split-cycle increases (Fig 6), and this is mainly caused by the higher exergy destruction taking place in the recuperators.

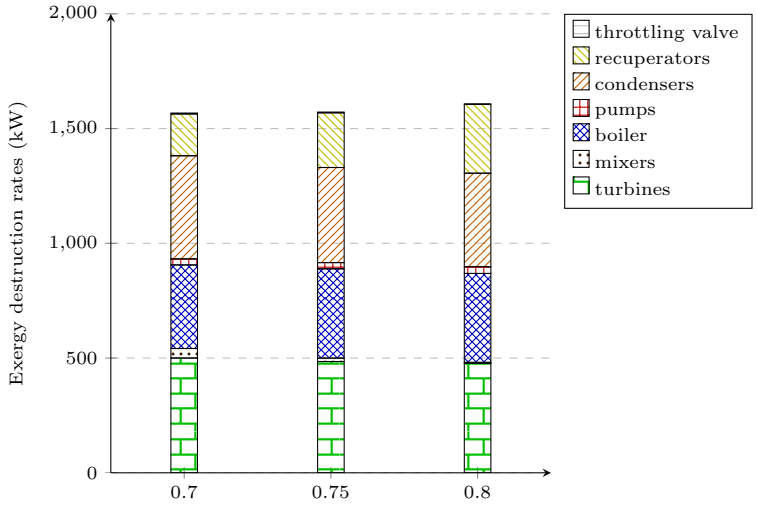

Figure 6: Exergy destruction sorted by processes, with three different ammonia concentrations (0.7, 0.75, 0.8)

The variations of the exergy flows and destruction for the three cases are shown in Table 5 – Table 7. Despite the different compositions, the exergetic efficiency of the turbines is unaffected. However, as the optimal flow rate of the working solution increases with the ammonia concentration, the amount of exergy entering and exiting the cycle components increases in all cases.

Table 5: Exergy inflows, outflows and destruction for an ammonia fraction of 0.7. Only the physical exergy flows are presented for clarity, as they are the only ones varying in the heat exchangers and turbines. The terms HP and LP stand for high-pressure and low-pressure, T for turbine, CD for condenser, PP for pump and REC for recuperator.

	HPT	LPT	Boiler	LPP	IREC	LPCD	REC1	RCD	RPP	REC2	REC3	LPP
Inflows, kW	3228	3063	9661	136	995	541	1544	342	303	736	392	121
Outflows, kW	3121	2671	9297	132	915	168	1468	266	292	719	382	109
Destruction, kW	108	393	364	3	80	373	76	77	11	17	9	12
Efficiency, %	82.2	80.1	89.9	70.7	80.2	10.3	86.0	2.4	71.5	52.6	59.5	72.8

Table 6: Exergy inflows, outflows and destruction for an ammonia fraction of 0.75. Only the physical exergy flows are presented for clarity, as they are the only ones varying in the heat exchangers and turbines. The terms HP and LP stand for high-pressure and low-pressure, T for turbine, CD for condenser, PP for pump and REC for recuperator.

	HPT	LPT	Boiler	LPP	IREC	LPCD	REC1	RCD	RPP	REC2	REC3	LPP
Inflows, kW	3223	2950	9572	208	1082	546	1618	472	421	1002	272	90
Outflows, kW	3081	2608	9183	205	1009	234	1481	369	406	981	264	81
Destruction, kW	142	342	389	3	72	312	137	102	16	21	8	9
Efficiency, %	82.2	80.1	89.9	70.9	76.8	10.2	78.7	2.5	71.4	59.7	65.3	72.7

It is worth noticing that a higher ammonia fraction of the working solution results in a smaller exergetic efficiency of all components operating at the low- and medium-pressure levels, except the ammonia-rich condenser. This is caused by the larger temperature gaps in the recuperators and condensers, which is evident in the case of the recuperator placed at the outlet of the turbine (REC1), with an efficiency drop of about 15 % points. On the contrary, the components operating at the high-pressure level, i.e. the rich and lean recuperators before the boiler, perform better, with an increase of the exergetic efficiency of about 20 % points.

Table 7: Exergy inflows, outflows and destruction for an ammonia fraction of 0.8. Only the physical exergy flows are presented for clarity, as they are the only ones varying in the heat exchangers and turbines. The terms HP and LP stand for high-pressure and low-pressure, T for turbine, CD for condenser, PP for pump and REC for recuperator.

	HPT	LPT	Boiler	LPP	IREC	LPCD	REC1	RCD	RPP	REC2	REC3	LPP
Inflows, kW	3485	3273	10151	368	1296	678	1930	610	550	1289	309	106
Outflows, kW	3368	2913	9764	366	1234	392	1722	488	531	1267	300	97
Destruction, kW	117	360	388	2	61	286	208	122	19	22	9	8
Efficiency, %	82.2	80.1	89.9	71.1	72.9	9.5	71.6	5.2	71.5	75.2	76.2	72.5

4.5. Entropy generation in the heat recovery system

For the preheater, boiler and superheater, Figure 7 shows the increase in generated entropy as heat is being transferred to the Kalina cycle. For a large part of the heat transfer the slope of the four curves is almost equal, indicating similar entropy generation. The major difference stems from the initial and final parts of the heat transfer. As previously discussed, the Kalina split-cycle offers a better match with the heat source around the pinch point, which is indicated here by the smaller rate of entropy generation at the beginning of the heat exchange.

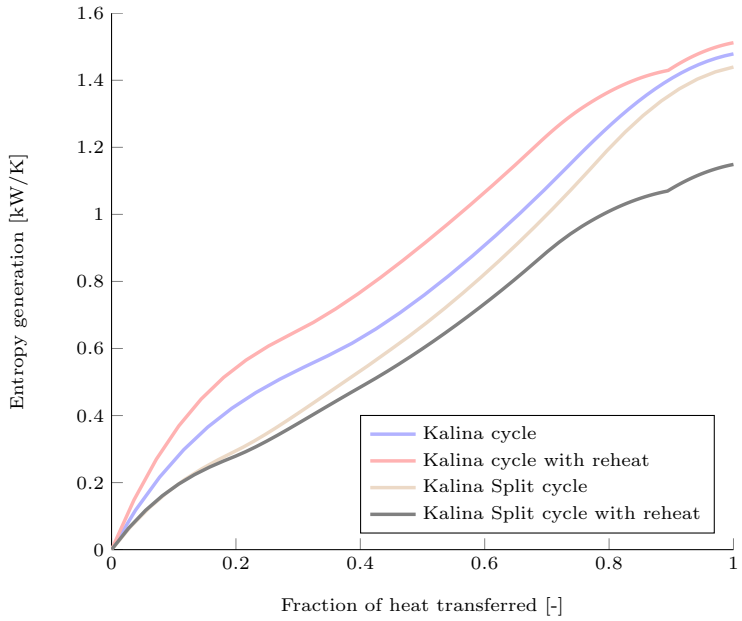

Figure 7: Entropy generation in preheater, boiler and superheater as a function of the total heat transfered. When reheating is used the heat related to the reheating is treated separately and is added at the ends of the curves

The addition of reheat increases the entropy generation in the case of the Kalina Cycle, and the main difference can again be seen at the start and end of the heat exchange. The Kalina cycle with reheat operates at a lower pressure: this results in a larger entropy generation at the start, but in a better match at the end. The overall entropy generation is therefore almost equal with and without reheat.

For the Kalina split-cycle, the opposite conclusions can be drawn, since the addition of reheat results in a reduction in entropy generation. The reheat also improves the temperature matches at the end of the heat transfer, but has little effect on the allowable inlet pressure, because of the smoothing near the pinch point.

4.6. Recommendations

These analyses provide highlights on the behaviour of the Kalina split-cycle in different environmental conditions. They suggest that integration opportunities of this power cycle exist for low- and medium-temperature waste heat recovery, and for different cooling water conditions. The Kalina Split Cycle is more

exergy-efficient when the heat source outlet temperature is low, and when the difference between the heat source inlet and outlet temperatures is large, as for conventional power cycles.

The results indicate that the process can provide near-optimum efficiencies across a large range of process parameters, due to the large number of parameters available for adjustment. This is for example seen by the results in Table 4, where Cases 7 and 8, yield very similar power outputs under similar boundary conditions, while the optimum design parameters found are not entirely similar (dissimilar high pressure level, but similar medium- and low-pressure ranges, as well as ammonia fraction).

In general, the different findings from this work highlight the following trends, which could be used as guidelines for further integration, and possibly for improving the exergetic efficiency in such power cycles (Table 8).

Table 8: Trends of the Kalina split-cycle

	T_{cw} ↘	T_{34} ↘	T_{37} ↘	$\dot{m}$ ↗
Ammonia mass flowrate	→	↘	↗	↗
High-level pressure	→	↘	↗	-
Medium level-pressure	↘	↘	→	↗
Low-level pressure	↘	↘	→	↗
Ammonia mass fraction	↗	↘	→	↗
Boiler destruction	↗	↘	↗	↗
Boiler efficiency	↗	↘	↘	→
Turbine destruction	↗	↘	→	↗
Turbine efficiency	↗	↘	→	→
Exergy efficiency	↗	↘	↗	↗ ↘

A lower cooling water temperature (T_{cw} ↘) allows for a lower condensation pressure of the ammonia-water solution and therefore a higher ammonia fraction. The medium- and low-pressure levels can be decreased: this implies that the average temperature of heat rejection is decreased, which would have beneficial effects on the thermal efficiency (i.e. greater power generation from the turbines). Different cooling water temperatures have a significant impact on the net power production, which increases by about 15 % when the cold reservoir is at 5 °C instead of 35 °C. Such trends are expected for power cycles.

A lower heat source temperature (T_{34} ↘), for the same exhaust temperature (T_{37}), implies that the amount of waste heat available for power generation decreases. The flow rate of the working solution should therefore be reduced, and this causes a drop in the exergy destruction in the boiler and turbines, as well as in the complete cycle. Similarly, the boiler and turbine exergetic efficiencies decrease, as a consequence of a lower temperature at the outlet of the boiler and at the inlet of the turbines.

A lower exhaust temperature (T_{37} ↘) results in a greater uptake of waste heat, and this allows for a higher flow rate of the working solution. The boiler pressure can as well be increased to reach the same temperature difference at the pinch point than in the baseline case, and this leads to a greater power output from the turbines. It is worth mentioning that: (i) the heat source temperature and superheating approach are maintained constant, the turbine inlet temperature is therefore fixed, and this explains why the turbine efficiency and destruction do not vary, (ii) the heat exchange in the boiler takes place over a larger range of temperatures, resulting in greater exergy destruction in this component, and (iii) the low- and medium-level pressure levels do not vary, as the ammonia concentration is nearly constant.

Regarding the different trends of the Kalina split-cycle, and the outcomes from the different steps of the analysis, two different optimisation strategies can be followed when integrating such a power cycle based on an ammonia-water mixture:

- enabling a high turbine inlet pressure (around 125–130 bar) and a high ammonia fraction (0.75–0.8); or
- enabling a low turbine outlet pressure and a low ammonia fraction (0.6–0.7).

The presence of these two strategies makes it difficult to recommend an explicit optimal operating range for a specific application, as there are two sets of conditions that can yield near-optimum solutions. The presented ranges are then given as guiding suggestions. In low- and medium-temperature waste heat

recovery applications, and for moderate cooling water temperatures ($T_{cw} \simeq$ 15-20 °C), the optimum low- and medium-pressure levels are in the ranges 3–4 bar and 9–11 bar, respectively. The optimal high-pressure level is generally about 120–130 bar, and may be decreased with smaller temperatures of the heat source or of the allowable rejection temperature.

At higher heat source temperatures than the ones investigated in this paper, the pressure may become a limiting factor. Both the Kalina cycle and Kalina split-cycle were already operating at pressures of 150 and 125 bar, respectively, which is significantly higher than the operating pressure of the Organic Rankine Cycle proposed by Bombarda et al. [5]. Furthermore, the high concentration of ammonia in the rich stream of the Kalina split-cycle results in a critical pressure of only 149 bar. Since the operating pressure of the base Kalina cycle is higher, it is expected that the Kalina split-cycle could also reach a scenario where the rich stream is in a super-critical state. This does not influence the working principle of the Kalina split-cycle, but may further complicate the cycle design and operation. Such issues should be taken into account when applying the split-cycle to higher temperature heat sources.

Finally, practical integration may also be challenging, as using ammonia-water mixtures implies higher safety requirements. Regarding environmental aspects, ammonia-water mixtures do not have any global warming [31] or ozone depletion potentials [32] but may cause water eutrophication [33], soil acidification [34] and can affect the human health. However, the preliminary life cycle analyses on the waste heat recovery cycles suggest that the benefits of substituting electricity from the grid are more valuable than the possible harms caused by the components manufacturing and the use of an ammonia-water mixture. The exact benefits should be quantified for each specific site and location, as different facilities have different practical requirements, and different countries operate on different electricity mixes.

5. Conclusion

An alternative process configuration of the Kalina cycle, namely the Kalina split-cycle, was investigated in the present work. Design parameters such as the ammonia concentration of the working fluid, the turbine pressure and the splitting fractions of the mixing and separation sub-system were optimised by application of a genetic algorithm.

The conventional Kalina cycle and the Kalina split-cycle, with and without reheat, were compared by conducting an exergy analysis. The greatest thermodynamic performance is reached with the Kalina split-cycle with reheat, as the result of a lower turbine exhaust pressure and a higher boiler inlet temperature, compared with the conventional Kalina cycle. These benefits are achieved at the expense of a higher system complexity.

The irreversibilities taking place in this unique power cycle are smaller by 2.5 to 5.0 % compared to the reference Kalina cycle. The most significant reduction in exergy destruction is related to the the boiler: the temperature match between the heat source and receiver is improved, and this leads to a smaller entropy generation. The largest exergy destruction takes place in the turbines and the boiler, and the least exergy-efficient components are the condensers and the recuperators.

A sensitivity analysis on the boundary conditions, i.e. the cooling water and exhaust gas temperatures, was performed. The results suggest that the net power output is mostly sensitive to the cooling water and inlet temperature of the waste heat source, while the exergy efficiency is mostly affected by the latter. The components that display the highest variation in exergy destruction are the boiler and the low-pressure turbine, but the ones that display the greatest sensitivity in terms of exergy efficiency are the recuperators and condensers.

Acknowledgements

The authors wish to thank the Lighthouse Maritime Competence Centre (www.lighthouse.nu) for their financial support.

Appendix A. State points

Table of state points for the Kalina split-cycle with reheat, reproduced from [12]:

Table A.9: Thermodynamic state points (T, P, h, x, q) for the Kalina split-cycle with reheat. The terms sup stand for superheated, sub for subcooled, x for the ammonia mass fraction and q for the vapour fraction, in the case of a two-phase behaviour.

Point	$\dot{m}$ (kg/s)	T (°C)	P (bar)	h (kJ/kg)	x	q
1	3.6	194.8	101.7	1390	0.677	0.478
2	3.6	234.9	101.7	2134	0.677	1
3	3.6	330	101.7	2500	0.677	Sup
3′	3.6	281	36.6	2331	0.677	Sup
3″	3.6	330	36.6	2602	0.677	Sup
4	3.6	133.1	2.9	2185	0.677	Sup
5	3.6	73.4	2.9	1323	0.677	0.669
6	10.6	51.3	2.9	502	0.478	0.234
7	10.6	25	2.9	24	0.478	0
8	10.6	25.1	10.1	25	0.478	Sub
9	10.6	68.4	10.1	256	0.478	0.021
10	10.6	85.8	10.1	549	0.478	0.174
11	8.8	85.8	10.1	282	0.376	0
12	7.3	85.8	10.1	282	0.376	0
13	7	85.8	10.1	282	0.376	0
14	7	41.9	10.1	79	0.376	Sub
15	7	42	2.9	79	0.376	0
16	1.5	85.8	10.1	282	0.376	0
17	0.3	85.8	10.1	282	0.376	0
18	1.8	85.8	10.1	1817	0.965	1
19	1.4	85.8	10.1	1817	0.965	1
20	1.7	85.8	10.1	1559	0.867	0.832
21	1.7	60.3	10.1	1325	0.867	0.734
22	1.7	41.9	10.1	1087	0.867	0.597
23	1.7	30	10.1	337	0.867	0
24	1.7	33.1	101.7	357	0.867	Sub
25	1.7	80.8	101.7	591	0.867	Sub
26	0.4	85.8	10.1	1817	0.965	1
27	1.9	85.8	10.1	615	0.504	0.217
28	1.9	74.5	10.1	439	0.504	0.128
29	1.9	41.9	10.1	112	0.504	Sub
30	1.9	43.8	101.7	129	0.504	Sub
31	1.9	80.8	101.7	304	0.504	Sub
32	1.9	194.8	101.7	915	0.504	0
33	1.7	194.8	101.7	1909	0.867	1
34	35	346	2	815	-	-
35	35	287.3	2	749	-	-
36	35	217.7	2	672	-	-
37	35	127.7	2	574	-	-

References

[1] Tchanche BF, Lambrinos G, Frangoudakis A, Papadakis G. Low-grade heat conversion into power using organic Rankine cycles A review of various applications. Renewable and Sustainable Energy Reviews 2011;15(8):3963–79.

[2] Jonsson M, Yan J. Ammoniawater bottoming cycles: a comparison between gas engines and gas diesel engines as prime movers. Energy 2001;26(1):31–44.

[3] Victor RA, Kim JK, Smith R. Composition optimisation of working fluids for Organic Rankine Cycles and Kalina cycles. Energy 2013;55:114–26.

[4] Wang J, Dai Y, Gao L. Exergy analyses and parametric optimizations for different cogeneration power plants in cement industry. Applied Energy 2009;86(6):941–8.

[5] Bombarda P, Invernizzi CM, Pietra C. Heat recovery from Diesel engines: A thermodynamic comparison between Kalina and ORC cycles. Applied Thermal Engineering 2010;30(2-3):212–9.

[6] Marston CH. Parametric Analysis of the Kalina Cycle. Journal of Engineering for Gas Turbines and Power 1990;112(1):107–16.

[7] Nag P, Gupta A. Exergy analysis of the Kalina cycle. Applied Thermal Engineering 1998;18(6):427–39.

[8] Dejfors C, Svedberg G. Second Law Analysis of Ammonia-Water Power Cycle for Direct-Fired Cogeneration Application. International Journal of Applied Thermodynamics 1999;2(3):125–31.

[9] Jonsson M. Advanced power cycles with mixture as the working fluid (Doctoral Thesis). Ph.D. thesis; Department of Chemical Engineering and Technology, Energy Processes, Royal Institute of Technology, Stockholm, Sweden; 2003.
[10] Singh OK, Kaushik S. Energy and exergy analysis and optimization of Kalina cycle coupled with a coal fired steam power plant. Applied Thermal Engineering 2013;51(1-2):787–800.
[11] Kalina A. A Kalina cycle technology and its applications. American Institute of Chemical Engineers, New York, United States of America; 1986,URL: www.osti.gov.
[12] Larsen U, Nguyen TV, Knudsen T, Haglind F. Optimisation and system analysis of a kalina-split cycle for waste heat recovery on large marine diesel engines. Energy 2013;64:484–94.
[13] Marston C, Hyre M. Gas turbine bottoming cycles: Triple pressure steam vs. Kalina. Transactions of the ASME 1995;117(January):10–5.
[14] El-Sayed Y. Theoretical comparison of the Rankine and Kalina cycles. ASME publication, AES 1985;1:97–102.
[15] Mathworks . Matlab R2010b Documentation. Tech. Rep.; Massachusetts, The United States; 2010. URL: www.mathworks.se; accessed 26-April-2013.
[16] Aspen Technology . Aspen Plus – Modelling Petroleum Processes. Burlington, USA: Aspen Technology; 1999.
[17] Tillner-Roth R, Friend DG. A Helmholtz free energy formulation of the thermodynamic properties of the mixture {water+ammonia}. Journal of Physical and Chemical Reference Data 1998;27(1):63–96.
[18] Thorin E. POWER CYCLES WITH AMMONIA -WATER MIXTURES AS WORKING FLUID Analysis of Different Applications and the Influence of Thermophysical Properties. Ph.D. thesis; Royal Institute of Technology; 2000.
[19] Aspen Tech Massachusetts, USA . Aspen Plus Software Version 7.2. 2010. URL: http://www.aspentech.com.
[20] Bejan A, Tsatsaronis G, Moran M. Thermal Design & Optimization. New York, USA: John Wiley & Sons; 1996.
[21] Moran MJ, Shapiro HN. Fundamentals of Engineering Thermodynamics. 6th ed.; New York, USA: John Wiley & Sons; 2007.
[22] Szargut J, Morris D, Steward F. Exergy analysis of thermal, chemical, and metallurgical processes. New York, USA: Hemisphere; 1988.
[23] Szargut J. Chemical exergies of the elements. Applied Energy 1989;32(4):269–86.
[24] Morris DR, Szargut J. Standard chemical exergy of some elements and compounds on the planet earth. Energy 1986;11(8):733–55.
[25] Kotas TJ. Exergy concepts for thermal plant: First of two papers on exergy techniques in thermal plant analysis. International Journal of Heat and Fluid Flow 1980;2(3):105–14.
[26] Kotas TJ. Exergy Criteria of Performance for Thermal Plant: Second of two papers on exergy techniques in thermal plant analysis. International Journal of Heat and Fluid Flow 1980;2(4):147–63.
[27] Kotas TJ. The Exergy Method of Thermal Plant Analysis. Malabar, USA: Krieger Publishing; 1995.
[28] Szargut J. Exergy in the thermal systems analysis. In: Bejan A, Mamut E, editors. Proceedings of the NATO Advanced Study Institute on Thermodynamic Optimization of Complex Energy Systems; vol. 69 of *NATO Science Series*. Neptun, Romania: Kluwer Academic Publishers; 1998, p. 137–50.
[29] Turton R, Bailie R, Whiting W, Shaeiwitz J, Bhattacharyya D. Analysis, Synthesis and Design of Chemical Processes. Prentice Hall International Series in the Physical and Chemical Engineering Sciences; 4th ed.; Prentice Hall; 2012.
[30] Gerber L, Fazlollahi S, Maréchal F. A systematic methodology for the environomic design and synthesis of energy systems combining process integration, life cycle assessment and industrial ecology. Computers and Chemical Engineering 2013;.
[31] Solomon, S. and Qin, D. and Manning, M. and Chen, Z. and Marquis, M. and Averyt, K.B. and Tignor, M. and Miller, H.L. . IPCC Fourth Assessment Report: Climate Change 2007 (AR4). Tech. Rep.; Intergovernmental panel on climate change; 2007.
[32] Global Atmosphere Watch Program . Scientific Assessment of Ozone Depletion: 2006. Tech. Rep.; World Meteorological Organization, United Nations; 2006.
[33] Heijungs, R. and Guine, J.B. and Huppes, G. and Lankreijer, R.M. and Udo de Haes, H.A. and Wegener Sleeswijk, A. and Ansems, A.M.M. and Eggels, P.G. and Duin, R. van and Goede, H.P. de . Environmental life cycle assessment of products: guide and backgrounds. Tech. Rep.; Institute of Environmental Sciences, CML, Leiden; 1992.
[34] Huijbregts, Mark A. J. . Priority assessment of toxic substances - development and application of the multi-media fate, exposure and effect model uses-lca. Tech. Rep.; Interfaculty Department of Environmental Science, Faculty of Environmental Sciences; 1999.